

**VOLATILE STABILITY MODELING OF LUNAR PITS AND CAVES.** A. X. Wilcoski<sup>1</sup>, P. O. Hayne<sup>1</sup>, and C. M. Elder<sup>2</sup> <sup>1</sup>University of Colorado, Boulder, CO, <sup>2</sup>Jet Propulsion Laboratory, California Institute of Technology (andrew.wilcoski@colorado.edu).

**Introduction:** Much of the motivation behind present-day lunar exploration centers around an interest in lunar volatiles from both a scientific and a resource utilization perspective. Since its existence has been established in recent decades, much of the work relating to lunar water ice has focused on determining what type of environments are most favorable for its stability and sequestration. Lunar collapse pits (Fig. 1), especially those connected to caves, have been suggested as environments that could store and protect ice to the benefit of future landed missions [1,2,3].

At high latitudes, collapse pits form effective Permanently Shadowed Regions (PSRs) due to their steep-walled geometry. PSRs are notable because some PSRs remain cold enough year-round to allow ice to be thermally stable for billions of years [4]. If ice were to accumulate in a cave system connected to a pit, the cave would provide added protection from potentially destructive surface processes, such as micrometeoroid bombardment. [5] detected several hundred pits on the lunar surface, some of which showed evidence of being connected to caves or overhangs, suggesting these features may be relatively common on the Moon. The majority of these pits were found in impact melt ponds within crater interiors, which implies that these pits should be able to form at any latitude [1,2].

In this work, we characterize the thermal environments within pits and caves as they vary with latitude and pit geometry using a 3D thermal model. We use the thermal model output to explicitly model water transport and ice stability within lunar pits and caves. Our results allow us to estimate the escape rates of water for these environments and determine whether ice deposits are expected to exist within lunar pits and caves.

**Thermal Model:** We develop and validate a 3D thermal model to calculate surface temperatures over time for a variety of different pit geometries at given latitudes. The model is initialized with a 3D surface composed of triangular facets of variable size. The model computes surface temperatures on each facet through time by balancing direct insolation, multiple-scattering of visible and infrared radiation, 1D subsurface heat conduction behind each facet, and infrared emission. The model also considers the effects of terrain shadowing.

**Volatile Transport Model:** We model the transport of water molecules within various pit geometries to evaluate the stability of water ice therein. Because of the Moon's relatively low gravity and the short length-

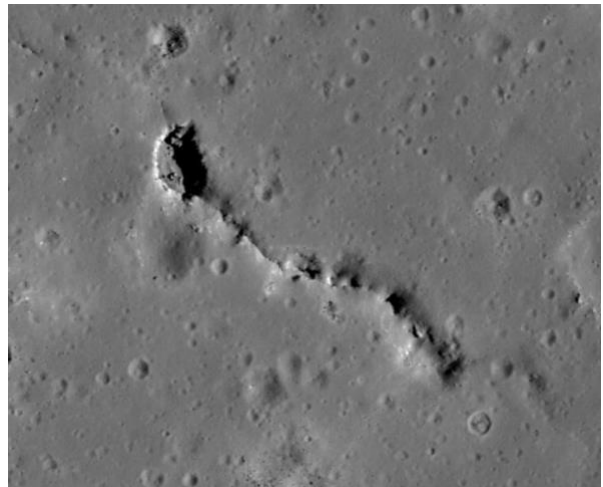


**Figure 1** Elliptical pit connected to a fracture/depression at 6.36° N, 119.93° E. LROC image M128509025RE (NASA/GSFC/ASU)

scales of lunar impact melt pits (~10 m [5]) the ballistic trajectories of water molecules within these 3D pit geometries can be approximated as straight lines. Therefore, water transport within pits can be modeled by analogy with a radiative process, where the mass exchange of water is analogous to the multiple-scattering of radiative energy between geometric facets. We initialize the volatile model with an arbitrary surface density of water across facets and then allow the model to evolve through time. The sublimation rate of water on each facet is determined by the facet temperature given by the 3D thermal model. The volatile transport model allows us to calculate the net rate of ice loss from a pit, which is equivalent to the rate of vapor supply necessary to maintain an ice deposit within a given pit. It also allows us to determine where ice is most stable within a single geometry (e.g., a pit or its connected cave).

**Results and Conclusions:** Figure 2 shows surface temperatures at local noon output by the 3D thermal model for a cylindrical pit with an attached cave at 80° S latitude. The surface facets along the poleward pit rim are directly illuminated by the sun have the highest temperatures. The majority of facets within the pit are in shadow. The primary energy source controlling the temperatures of shadowed facets is scattered and emitted infrared radiation from other facets. The steep-walled nature of pits and caves results in very efficient multiple-scattering of radiation, causing their interior temperatures to be relatively uniform at any given time.

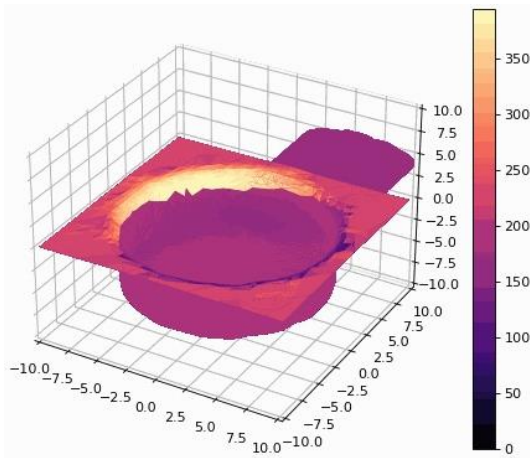


**Figure 2** Modeled surface temperatures of a cylindrical pit with attached cave. The colorbar units are degrees Kelvin.

Figure 3 shows the mean temperatures across all facets within a pit and the connected cave over the course of a lunar day. The dashed lines show mean temperatures for the geometry shown in Figure 2, while the solid lines show mean temperatures for the same geometry when it is placed within the PSR of a crater at the same latitude (see Fig. 4). We refer to the latter geometry as ‘doubly shadowed’. The non-PSR pit and cave temperatures are considerably higher than those of the doubly shadowed pit and cave. In general, most pit geometries we tested that are not doubly shadowed have temperatures too high to be favorable for long-term ice stability.

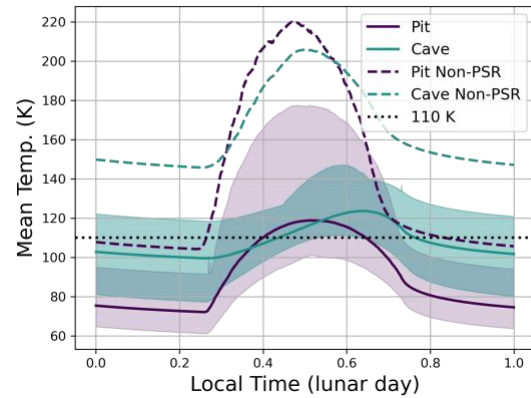


**Figure 3** Spatial mean temperature for a pit (purple) and its attached cave (blue) over a lunar day. The shaded regions show maximum and minimum temperatures for the doubly shadowed pit and cave. See text for details.

Figure 4 shows ice surface density at the beginning and end of a 20-year volatile model run for a doubly shadowed pit/cave system at 80° S latitude. The model run is initialized with a constant ice surface density across all facets within the pit/cave and no ice outside the pit/cave. By the end of the model run, about 15% of the original ice mass has escaped. The remaining ice has moved to where it is most stable, mainly on the pit floor and the cave roof. The net rate of ice loss from the pit/cave is rapid at first and then stabilizes as a model run continues. By the end of the 20-year model run the pit/cave is losing ice at a rate of  $1.5 \times 10^{-7} \text{ kg s}^{-1}$ .

**References:** [1] Lee P. (2018) *LPSC 49* Abstract #2083. [2] Avent W. and Lee P. (2021) *LPSC 52*, Abstract #2548. [3] Hooper, D. M. et al. (2021) *LSSW XII*, Abstract #8025. [4] Watson K. et al. (1961) *JGR*, 66, 1598. [5] Wagner R. V. and Robinson M. S. (2014) *Icarus*, 237, 52-60.

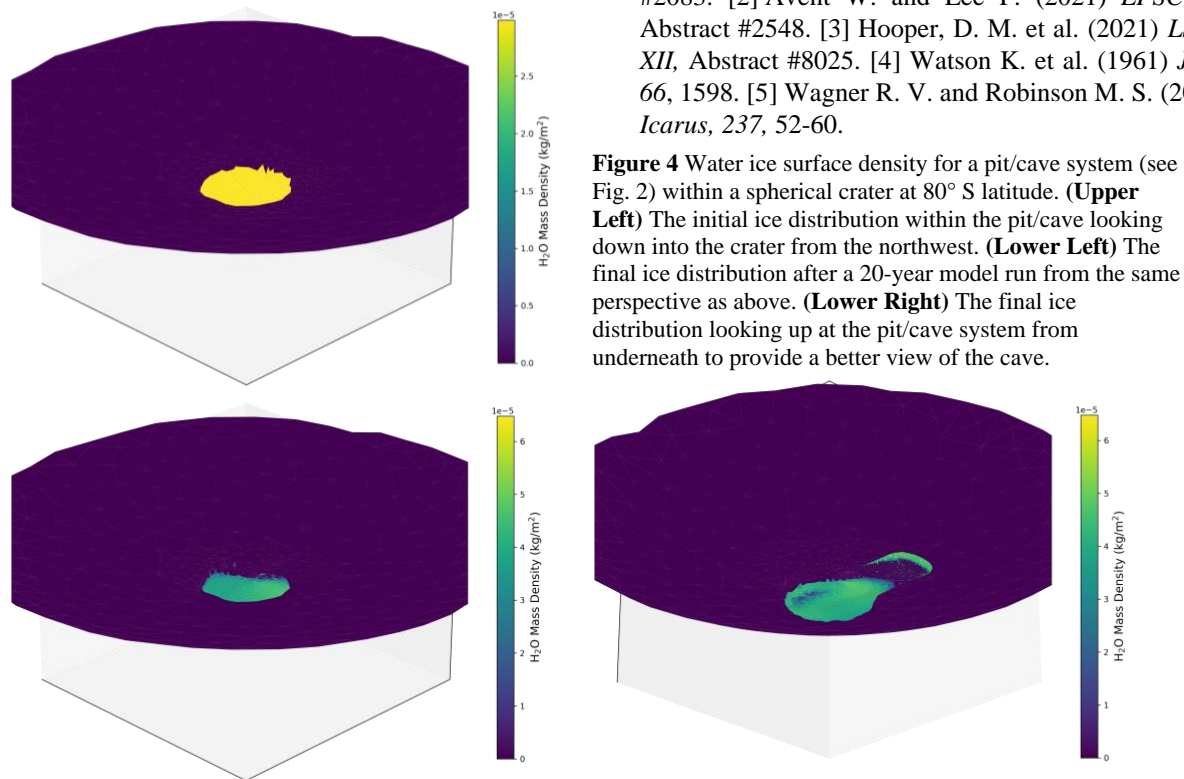


**Figure 4** Water ice surface density for a pit/cave system (see Fig. 2) within a spherical crater at 80° S latitude. (**Upper Left**) The initial ice distribution within the pit/cave looking down into the crater from the northwest. (**Lower Left**) The final ice distribution after a 20-year model run from the same perspective as above. (**Lower Right**) The final ice distribution looking up at the pit/cave system from underneath to provide a better view of the cave.